International Journal of Mass Spectrometry 284 (2009) 47–56

Contents lists available at ScienceDirect

International Journal of Mass Spectrometry

journal homepage: www.elsevier.com/locate/ijms

Analysis of archaeological triacylglycerols by high resolution nanoESI, FT-ICR MS and IRMPD MS/MS: Application to 5th century BC–4th century AD oil lamps from Olbia (Ukraine)

Nicolas Garnier[a,b], Christian Rolando[a], Jakob Munk Højte[c], Caroline Tokarski[a,*]

[a] Chimie Organique et Macromoléculaire, UMR CNRS 8009, and Protéomique, Modifications Post-traductionnelles et Glycobiologie, IFR 147, Université des Sciences et Technologies de Lille, 59655 Villeneuve d'Ascq Cedex, France
[b] SARL Laboratoire Nicolas Garnier, 63270 Vic le Comte, France
[c] Danish National Research Foundation's Centre for Black Sea Studies, University of Aarhus, 8000 Aarhus C, Denmark

ARTICLE INFO

Article history:
Received 16 March 2008
Received in revised form 15 February 2009
Accepted 6 March 2009
Available online 20 March 2009

Keywords:
Lipidomics
Triacylglycerol
FT-ICR MS
InfraRed multiphoton dissociation
Archaeological oil lamp

ABSTRACT

This work presents the precise identification of triacylglycerols (TAGs) extracted from archaeological samples using a methodology based on nanoelectrospray and Fourier transform mass spectrometry. The archaeological TAG identification needs adapted sample preparation protocols to trace samples in advanced degradation state. More precisely, the proposed preparation procedure includes extraction of the lipid components from finely grinded ceramic using dichloromethane/methanol mixture with additional ultrasonication treatment, and TAG purification by solid phase extraction on a diol cartridge. Focusing on the analytical approach, the implementation of "in-house" species-dependent TAG database was investigated using MS and InfraRed Multiphoton Dissociation (IRMPD) MS/MS spectra; several vegetal oils, dairy products and animal fats were studied. The high mass accuracy of the Fourier transform analyzer (Δm below 2.5 ppm) provides easier data interpretation, and allows distinction between products of different origins. In details, the IRMPD spectra of the lithiated TAGs reveal fragmentation reactions including loss of free neutral fatty acid and loss of fatty acid as α,β-unsaturated moieties. Based on the developed preparation procedure and on the constituted database, TAG extracts from 5th century BC to 4th century AD Olbia lamps were analyzed. The structural information obtained succeeds in identifying that bovine/ovine fats were used as fuel used in these archaeological Olbia lamps.

1. Introduction

The organic material contained in archaeological ceramics represents an essential evidence of human activities through years. Coarse wares, and particularly oil lamps, are typologically well-known materials, however, most of the chemical studies are devoted to lamp ceramic composition [1] and since the pioneering work of Passi et al. [2], few studies have investigated the identification of lamp fuels [3–6]. Identifying the ancient fuel origins raises the question of methodologies and chemical arguments for the identification of natural fats. Taking example of beeswax identification, analysis are focusing on association of odd-numbered /n/-alkanes and /n/-alkenes, even-numbered cerides derived from palmitic acid and 15-hydroxypalmitic acid, and hydrolyzed fatty acids and long chain /n/-alcohols [7]. However, the other fatty materials (vegetal oils, animal fats) present a simpler and very similar chemical constitution dominated by triacylglycerols, which entangles the possibility of direct identification based on fatty acids preserved in the potsherds. So fatty material identification is actually based either on Gas Chromatography Mass Spectrometry (GC–MS) with $\delta^{13}C$ isotope ratio analysis [4] or on oxygenated degradation products analysis using GC–MS [8].

Considering more particularly the archaeological context, it can be underlined that triacylglycerols, i.e., main component of vegetal oils and mammal fats [9], are sensitive to hydrolysis of the ester functions or oxidation of the double bonds [10]. And, despite the application of chromatography-based methods for TAG analysis [11–24], their lability makes their detection very difficult in archaeological material. To the best of our knowledge, only two references expose identification of animal fats mixed with olive oil [5] and beeswax [25] in archaeological samples

* Corresponding author at: Université des Sciences et Technologies de Lille, UFR de Chimie, Bâtiment C4, UMR CNRS 8009, Chimie Organique et Macromoléculaire, 59655 Villeneuve d'Ascq Cedex, France. Tel.: +33 3 20 33 64 33; fax: +33 3 20 33 61 36.
E-mail address: Caroline.Tokarski@univ-lille1.fr (C. Tokarski).

1387-3806/$ – see front matter © 2009 Elsevier B.V. All rights reserved.
doi:10.1016/j.ijms.2009.03.003

using HPLC-APCI-MS. To obtain more information on native TAGs from archaeological samples, a mass spectrometry-based method using nanoelectrospray source was proposed [7,26–29] allowing pertinent determination of biological sources. We describe here the application of the developed methodology implemented with the high mass accuracy and high resolution of Fourier Transform Ion Cyclotron Resonance analyzer (FT-ICR-MS) to analyze invisible residues preserved as impregnations in the inner porous side of ancient oil lamps from Olbia (Ukraine). Identification of archaeological TAGs requires extraction, purification and analysis protocols specifically adapted to trace samples in advanced degradation state. Consequently, the proposed work includes a procedure based on preliminary extraction step of the lipidic components using dichloromethane/methanol mixture as extraction solvent with ultrasonication treatment; this procedure was applied to ceramic finely crushed with an electrical mill. Additionally, a purification step was added using a diol cartridge. The analytical approach is based on the implementation of "in-house" species-dependant TAG database using MS and InfraRed Multiphoton Dissociation (IRMPD) MS/MS spectra, particularly; it reveals fragmentation reactions allowing the precise determination of each fatty acid moiety. The developed protocol and the species-dependant TAG database were finally used to analyze and identify precisely the ancient lamps TAGs.

2. Materials and methods

2.1. Solvents and reagents

All organic analytical grade solvents were purchased from VWR (VWR-France, Fontenay-sous-Bois, France), and lithium chloride (>98%) from Sigma (St-Quentin Fallavier, France). The silica-based diol phase Sep-Pak SPE cartridges were purchased from Waters (Guyancourt, France).

2.2. Authentic modern samples

The modern products constituting the database were chosen according to the vegetal species cultivated and imported, and the animals bred in North-Mediterranean regions (Table 1). The adipose fats were sampled from freshly slaughtered ox, veal, lamb and pork, from subcutaneous tissues and from solid fatty tissues enveloping kidneys. Lanolin, a product made regionally from lamb wool, was bought in an herbalist in the suk al-Gouri in Cairo (Egypt).

Table 1
Studied modern reference material details and origins.

Biological source	Taxonomy	Origin
Animal fats		
Ox, subcutaneous adipose tissue	*Bos taurus*	Auvergne, France
Ox, yellow solid fat arrounding kidneys	*Bos taurus*	Auvergne, France
Veal, subcutaneous adipose tissue	*Bos taurus*	Auvergne, France
Veal, white solid fat arrounding kidneys	*Bos taurus*	Auvergne, France
Lamb, subcutaneous adipose tissue	*Ovis aries*	Auvergne, France
Lamb, white solid fat arrounding kidneys	*Ovis aries*	Auvergne, France
Pig, subcutaneous adipose tissue	*Sus scrofa*	Auvergne, France
Pig, white solid fat arrounding kidneys	*Sus scrofa*	Auvergne, France
Sheep, lanoline	*Ovis aries*	Local market, Cairo, Egypt
Duck, subcutaneous adipose tissue	*Anas platyrhynchos*	Auvergne, France
Vegetal oils		
Almond sweet oil, cold-pressed	*Prunis amygdalus*	Damascus, Syria
Argan oil, cold-pressed, traditional handicraft	*Argania spinosa*	Local market, Marocco
Castor oil, cold-pressed	*Ricinus communis*	Artisan Moulinier, Beaulieu, France
Chamomile oil, cold-pressed	*Chamaemelum nobile*	Damascus, Syria
Grape seed oil, cold-pressed	*Vitis vinifera*	Artisan Moulinier, Beaulieu, France
Hazelnut oil, cold-pressed	*Corylus avellana*	Artisan Moulinier, Beaulieu, France
Laurel oil, cold-pressed	*Laurus nobilis*	Damascus, Syria
Lettuce oil, cold-pressed	*Lactuca sativa*	Damascus, Syria
Linseed filtered clarified oil, cold-pressed	*Linum usitatissimum*	Kremer, Germany
Mint oil, cold-pressed	*Mentha sp.*	Damascus, Syria
Mustard, cold-pressed	*Brassica nigra*	Artisan Moulinier, Beaulieu, France
Nigella oil, cold-pressed	*Nigella sativa*	Damascus, Syria
Nut oil, cold-pressed	*Juglans regia*	Local made (F)
Olive, mesocarp of fruits	*Olea europaea*	Nyons, France
Olive oil, cold-pressed	*Olea europaea*	Commercial oil, Toscana, Italy
Olive oil, cold-pressed	*Olea europaea*	Nyons, France
Palm oil, cold-pressed	*Elaeis guinensis*	Red non-refined oil, Senegal
Pine kernel oil, cold-pressed	*Pinus pinea*	Artisan Moulinier, Beaulieu, France
Pistachio oil, cold-pressed	*Pistacia vera papaver*	Artisan Moulinier, Beaulieu, France
Poppy seed oil, cold-pressed	*Papaver somniferum*	Local market, Vic le Comte, France
Rapeseed oil, cold-pressed	*Brassica napus*	Artisan Moulinier, Beaulieu, France
Rocket/Arugula oil, cold-pressed	*Eruca sativa*	Damascus, Syria
Safflower oil, cold-pressed	*Carthamus tinctorius*	Artisan Moulinier, Beaulieu, France
Sesame oil, cold-pressed	*Sesamum indicum*	Artisan Moulinier, Beaulieu, France
Sesame seed	*Sesamum indicum*	Local market, India
Wheat germ oil, cold-pressed	*Triticum vulgare*	Damascus, Syria
Dairy products		
Cow, milk	*Bos taurus*	Auvergne, France
Cow, raw milk cheese (Saint-Félicien)	*Bos taurus*	Local market, Vic le Comte, France
Ewe, raw milk cheese (Ossau-Iraty)	*Ovis aries*	Local market, Vic le Comte, France
Goat, raw milk cheese	*Capra hircus*	Local market, Vic le Comte, France
Camel, milk	*Camelus dromedarius*	Petra, Jordan

Fig. 1. Olbia lamp fragment, noted X4, analyzed using the mass spectrometry-based procedure described in this work.

The details and origins of vegetable oils, including olive, argan or sesame, and dairy products including cow, goat or ewe milk cheese are detailed in Table 1.

2.3. Archaeological samples

Nine lamps were selected amongst the material excavated from the settlement of Olbia (Ukraine) by J. Munk Højte (Aarhus University, Danish National Research Foundation's Centre for Black Sea Studies, Denmark). The old city is located strategically on a widely extended shelf by the estuary of the Bug River, along the shore of the Black Sea. The studied sector consists on the living quarter of the Lower City, occupied from the 5th century BC to the 4th century AD. The lamps did not present any visible organic residues on their inner side as can be observed in Fig. 1 showing the lamp noted X4; the external diameter was approximately 8.5 cm. The samples were firstly analyzed using pyrolysis-high resolution gas chromatography coupled to mass spectrometry (Electron Impact source) (THM-HRGC-EIMS, data not shown) in the presence of tetramethylammonium hydroxide (TMAH) to detect the presence of organic matter, and especially fatty acids. Because of the high degree of preservation of their lipidic compounds, six samples were chosen for analysis.

2.4. TAG extraction and purification from modern adipose tissues, vegetable oils and dairy products

2.4.1. TAG extraction and purification from modern adipose tissues and dairy products

The extraction protocol was adapted from a methodology described by Folch et al. [30]. The tissue or the dairy product (~1 g) was homogenized in a mixture of dichloromethane/methanol 1:1, v/v (20 mL) and placed in ultrasonic bath for 20 min. The mixture was filtered on 0.22 μm filter and potassium chloride solution (0.12 M, 5 mL) was added to the filtrate. After extraction and separation of the two phases by centrifugation, the organic layer was dried over $MgSO_4$, evaporated to dryness under a nitrogen stream at 40 °C. A 2 mg aliquot of the residue was dissolved in dichloromethane (1 mL). The TAGs were purified by fractionation on a Sep-Pak diol cartridge beforehand rinsed with cyclohexane (4 mL) [31,32]. The lipid extract (100 μL) was deposed and the TAGs eluted 3 times by 2 mL of a mixture of cyclohexane/dichloromethane/Et_2O (89:10:1, v/v/v). Other polar lipids were eluted two times by 2 mL of dichloromethane/methanol (2:1, v/v) and fatty acids by methanol (5 mL). The first fraction was evaporated to dryness, the residue dissolved in 1 mL dichloromethane/methanol (1:1, v/v).

2.4.2. TAG extraction and purification from vegetable oils

The liquid vegetal oils were diluted twice with dichloromethane in order to obtain solutions at 2 mg/mL. The TAGs were purified by fractionation on a Sep-Pak diol cartridge as detailed for modern adipose tissues and dairy products (see Section 2.4.1).

2.5. TAG extraction and purification from archaeological lamps

A fragment of approximately 1.0 g of each ceramic was crushed using an electrical mill (IKA A-11 basic) during 10 s. The powder was extracted twice with 5 mL dichloromethane/methanol (2:1, v/v), the organic phases was separated each time by centrifugation (10 min at 2500 rpm, then 20 min at 4100 rpm). The clear solution was evaporated to dryness under a nitrogen stream at 40 °C, then the TAGs were purified according the procedure described previously for adipose tissues using SPE on a diol-cartridge (see Section 2.4.1).

2.6. NanoESI-Qh-FT-ICR MS and MS/MS analysis

The purified TAG fractions, diluted with methanol (1/50, 5 μl), were cationized using lithium chloride solution (2% in methanol). The solution containing TAGs and lithium chloride was then diluted to 1/100 with methanol [29,32]. The samples were analyzed with an Apex Qe 9.4 T Fourier Transform Ion Cyclotron Resonance Mass Spectrometer (Bruker Daltonics, Bremen, Germany). The FT-ICR mass spectrometer is equipped with a nano-electrospray source. Detection was carried out in positive mode. A potential of 1.3 kV was applied on the needle (PicoTip Emitter, New Objective, Woburn, MA, USA). The detection The detection parameters were broadband detection, 512 K acquisition size, start mass at m/z 200 leading to 0.5243 s transient duration allowing theoretical resolution of 190,000 at m/z 400. Ions were accumulated in the hexapole during 1 s, and in the collision cell 0.01 s and 2 s, respectively, for MS and MS/MS. InfraRed Multiphoton Dissociation fragmentation mode was employed for MS/MS experiments using 20% of the laser power (CO_2 laser with 10.6 μm wavelength, high power 25 W laser) and 0.3 s IR pulse length. The spectra calibration was done using an external calibrant using single-point calibration and the spectra analysis was done manually.

3. Results and discussion

3.1. MS profiles of the lithiated TAG from modern materials

The MS and MS/MS profiles of purified TAGs from animal, dairy and vegetal fats diluted in a lithiated methanolic solution were investigated to create the species-dependant TAG database. The MS experiment allows distinguishing components according to their Equivalent Carbon Number (ECN), their unsaturation degree and the MS/MS profiles, completing the elucidation of the molecular structure of each compound. It has to be highlighted that the Fourier transform analyzer allows high mass accuracy providing easier data interpretation [33] and allowing identification of TAG modifications as for example relative to oxidative changes [34].

Considering more precisely the vegetal oils (Fig. 2), it can be noticed that most of modern references present a similar narrow distribution of TAGs from ECN 50 to ECN 54 with two or three patterns, each one separated by 26–28 amu. This is a direct consequence of the distribution of the constitutive fatty acids in oils, and the predominance of one acid in most of them, the oleic acid [9]. However, each vegetal oil species presents a singular

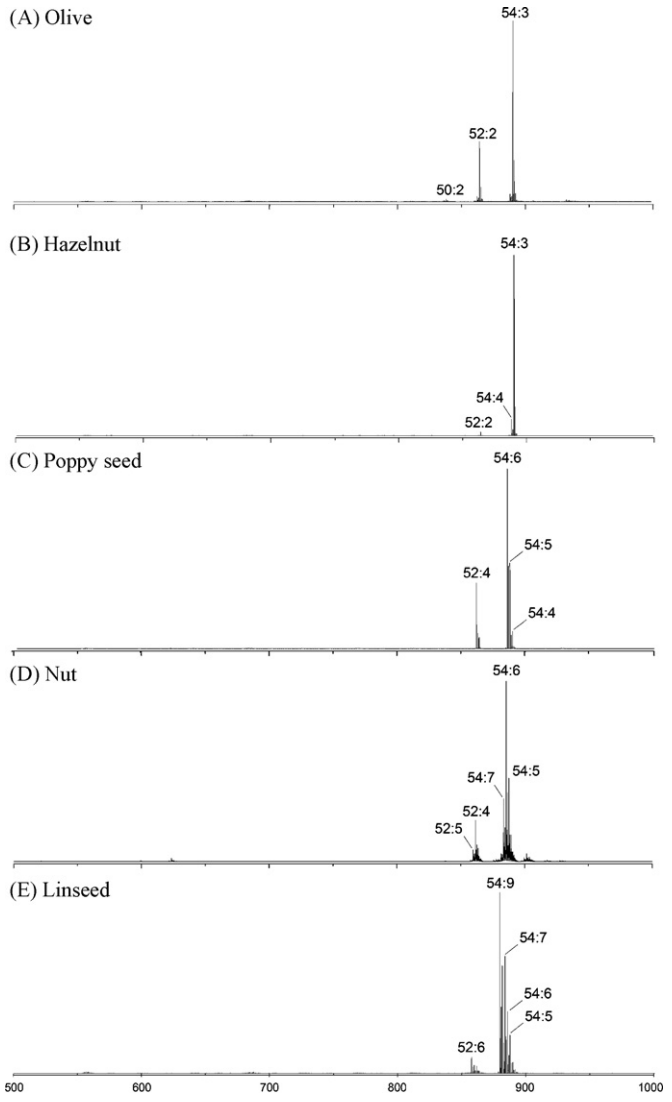

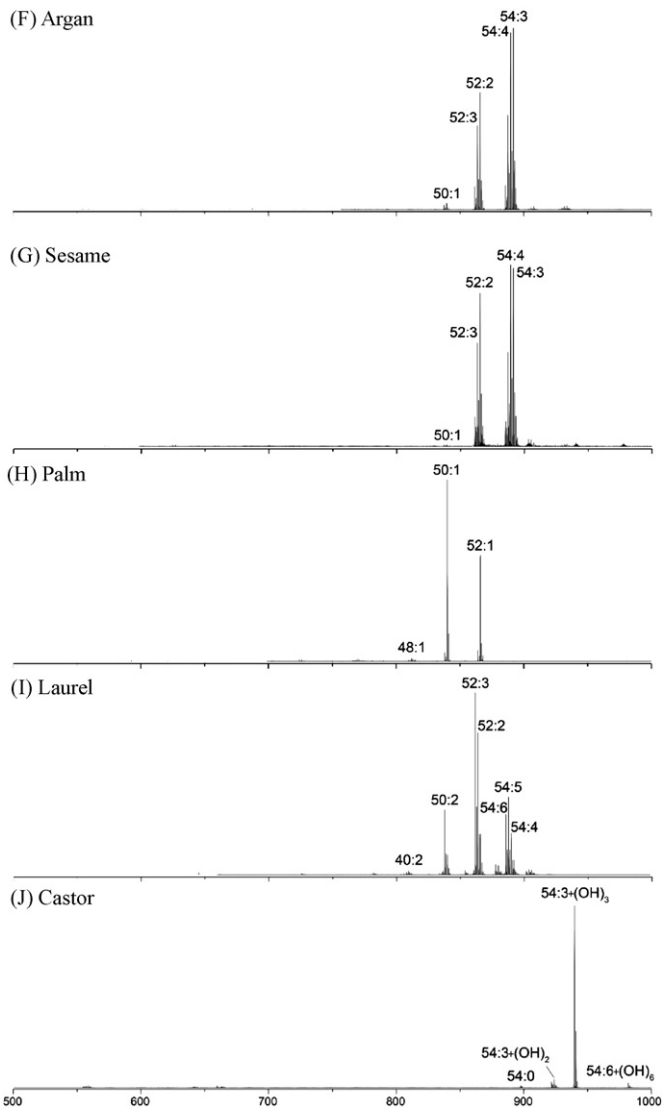

Fig. 2. MS profiles of the TAG fractions from several modern vegetal oils including (A) olive oil, (B) hazelnut oil, (C) poppy seed oil, (D) nut oil, (E) linseed oil, (F) argan oil, (G) sesame oil, (H) palm oil, (I) laurel oil and (J) castor oil.

Fig. 2. (*Continued*).

pattern which affords to discriminate and authenticate them. For example, the olive oil spectrum (Fig. 2(A)) is mainly dominated by ECN 52 and ECN 54. In details the major peaks are 54:3 and 52:2 which can be identified as TAG triolein OOO (see Table 2 for nomenclature and abbreviation details) and the TAG OOP. As other example, the presence of highly abundant acids such as lauric acid (abbreviation 12), palmitic acid (abbreviation P), or ricinoleic acid (abbreviation Ri) respectively in laurel (Fig. 2(I)), palm (Fig. 2(H)), and castor oils (Fig. 2(J)), gives very distinct patterns ranged from lower mass for the two first oils, e.g., ECN 40–54 (laurel) and ECN 48–52 (palm), to the higher mass for castor oil, e.g., ECN 54.

Considering the dairy products (Fig. 3), it can be observed that they are rich in palmitic, oleic (abbreviation P), stearic (abbreviation S), capric acids (abbreviation 10) and other saturated short-chain fatty acids in fewer amounts. This diversity induces a large distribution of TAGs from ECN 24 to ECN 54. The TAG 36:0 is the major one for cow (Fig. 3(A)), goat (Fig. 3(B)) and ewe milks (Fig. 3(C)) and the corresponding raw-milk cheeses. Their mass profiles are too similar to allow a direct distinction between bovine, ovine, and caprine dairy products, and a dedicated methodology has to be employed to discriminate the species origin [27]. All dairy products are charac-

Table 2
Nomenclature and mass of the fatty acid moieties lost during fragmentation of the TAGs.

Substituant name	Formula	Abbreviation	*n*:*i*	Mass
Capric acid	$C_{10}H_{20}O_2$	10	10:0	172.1457
Lauric acid	$C_{12}H_{24}O_2$	12	12:0	200.1770
Myristic acid	$C_{14}H_{28}O_2$	M	14:0	228.2083
Pentadecanoic acid	$C_{15}H_{30}O_2$	15	15:0	242.2240
Palmitoleic acid	$C_{16}H_{30}O_2$	Po	16:1	254.2240
Palmitic acid	$C_{16}H_{32}O_2$	P	16:0	256.2396
Heptadecenoic acid	$C_{17}H_{32}O_2$	17′	17:1	268.2396
Margaric acid	$C_{17}H_{34}O_2$	Ma	17:0	270.2553
Linoleic acid	$C_{18}H_{32}O_2$	Ln	18:2	280.2396
Oleic acid	$C_{18}H_{34}O_2$	O	18:1	282.2553
Stearic acid	$C_{18}H_{36}O_2$	S	18:0	284.2709
Nonadecenoic acid	$C_{19}H_{36}O_2$	19′	19:1	296.2709
Nonadecanoic acid	$C_{19}H_{38}O_2$	19	19:0	298.2866
Ricinoleic acid	$C_{18}H_{34}O_2$	Ri		298.2502
Arachidic acid	$C_{20}H_{40}O_2$	Ad	20:0	312.3022
Eicosatrienoic acid	$C_{20}H_{34}O_2$	20‴	20:3	306.2553
Eicosenoic acid	$C_{20}H_{38}O_2$	20′	20:1	310.2866
Heneicosanoic acid	$C_{21}H_{42}O_2$	21	21:0	326.3179

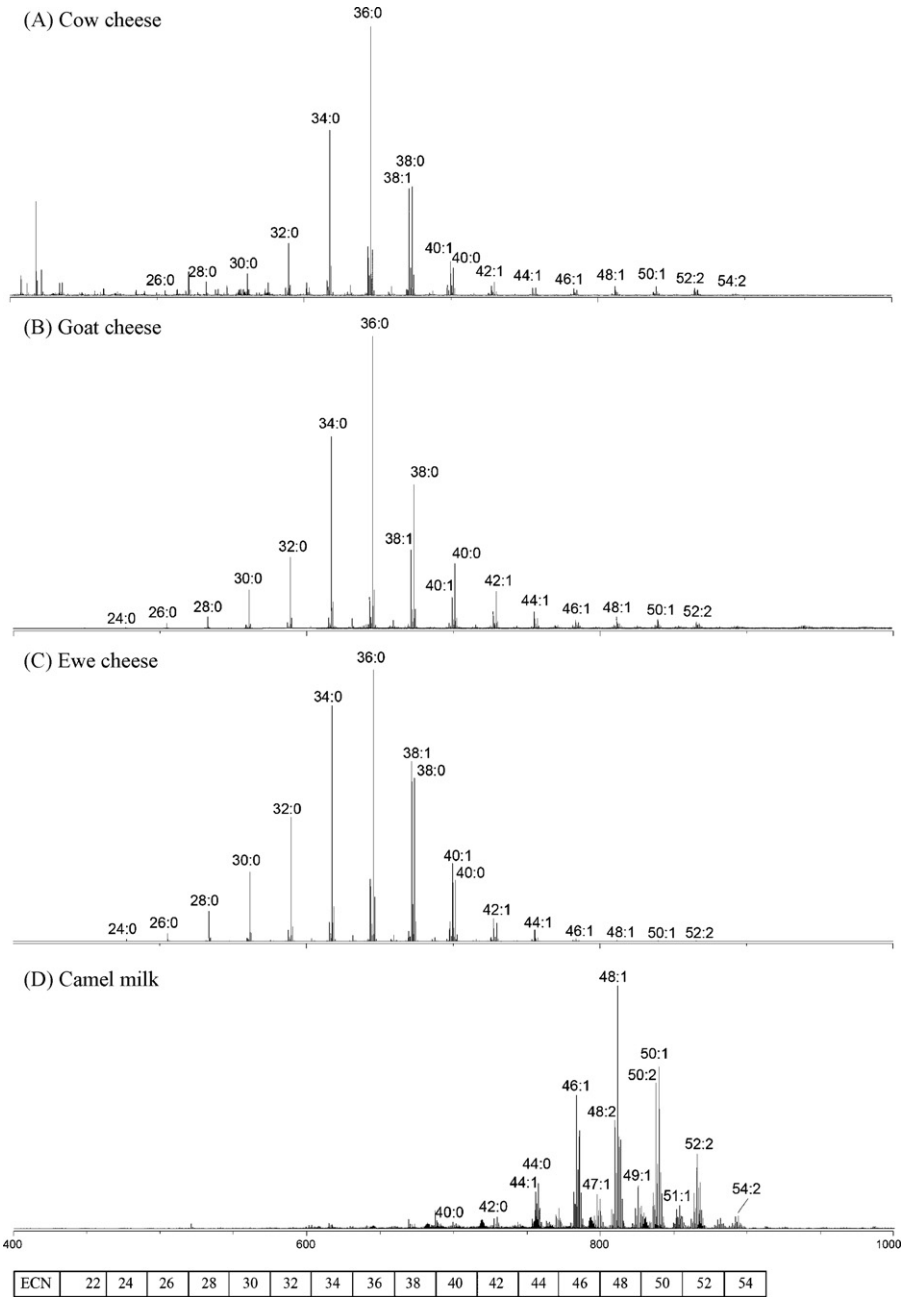

Fig. 3. MS profiles of the TAG fractions from several modern dairy products including (A) cow cheese, (B) goat cheese, (C) ewe cheese and (D) camel milk.

terized by the presence of smaller intercalated peaks corresponding to TAG containing one odd-number fatty acid. The analysis of the total fatty acids indicates isomers of penta-, hepta- and nonadecanoic acids for the main ones, including the linear isomer and their branched homologous compounds [35]. The relative proportion of such odd TAGs is particularly important for example for camel milk (Fig. 3(D)).

The mass profile of animal fats (Fig. 4) covers a broad mass range corresponding to TAGs with ECN from 46 to 54. The main marker is the TAG 52:2 for bovine (Fig. 4(A and B)), ovine (Fig. 4(C)), porcine (Fig. 4(D)), and duck species (Fig. 4(F)). Lanoline (Fig. 4(E)) consists of higher unsaturated TAGs, with the predominating TAGs 54:6 and 54:5. Bovine and ovine profiles present the alternation of abundant even-number TAG and of minor odd-number TAGs.

As observed for dairy products, odd-number fatty acids are markers of ruminant species (i.e., ox, cow, veal, lamb), mainly synthesized by bacteria present in the rumen (i.e., larger part of the reticulorumen and serves as the primary site for microbial fermentation of ingested feed) [35]. Porcine or duck fats are exempt of such compounds and consequently presents a narrower distribution. Except the discrimination of poultry and porcine against bovine and ovine fats, no further authentication can be suggested by the only MS analysis and more complete MS/MS study has to be investigated to obtain pertinent data.

Globally, it can be pointed out that compared to the methods using other ionization sources, the analysis of TAGs by nanoelectrospray mass spectrometry conduces to simpler spectra, and allows the detection of the unsaturated and saturated TAGs without in-source fragmentation.

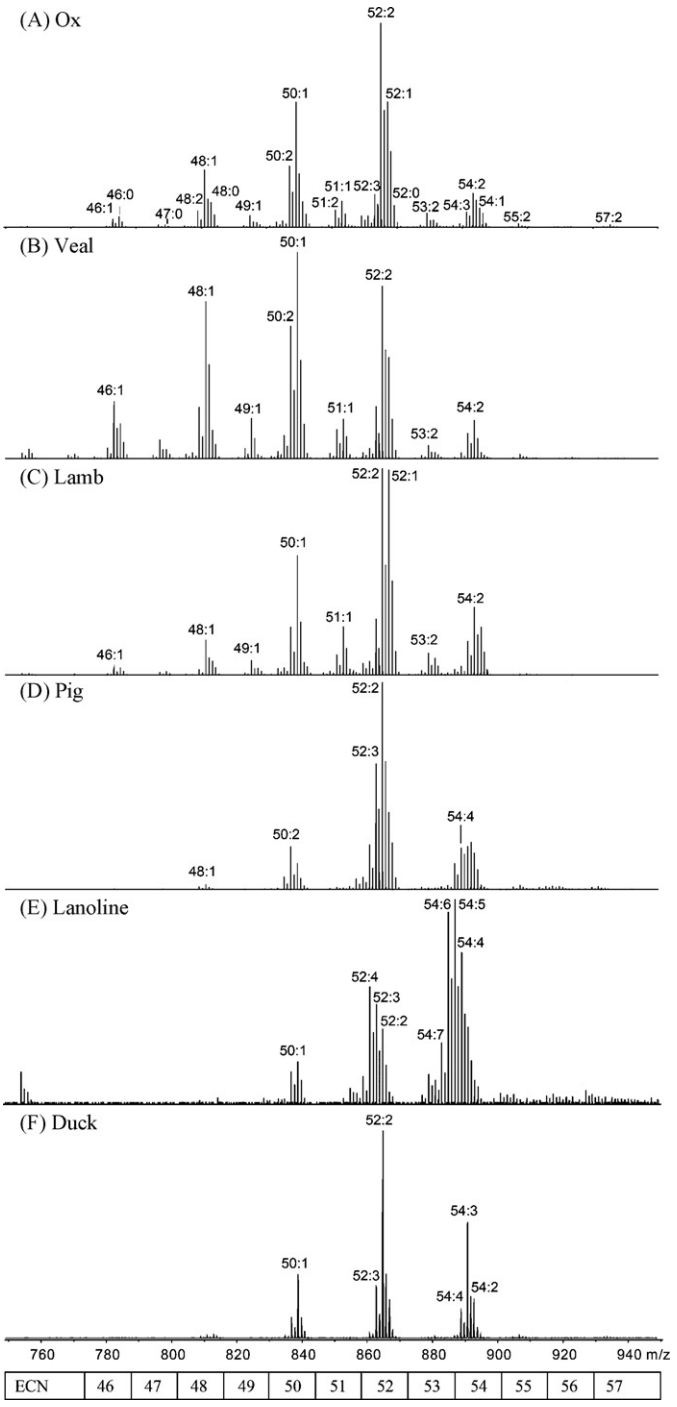

Fig. 4. MS profiles of the TAG fractions from several modern fats enveloping kidneys from (A) ox, (B) veal, (C) lamb, and (D) pig, from (E) lanoline and (F) subcutaneous adipose tissues from duck.

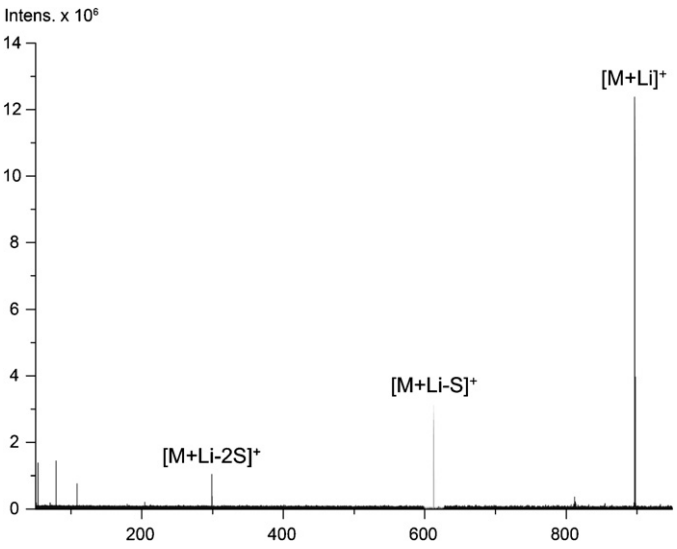

Fig. 5. IRMPD MS/MS profiles of the ion $[M + Li]^+$ at m/z 897.8466 from ox tallow TAGs extract corresponding to tristearin (54:0) and highlighting the loss of free fatty acid from the precursor ion and the fatty acid ion in the low mass range. The abbreviation details are specified in Table 2.

3.2. Structural elucidation of ox tallow triacylglycerols

3.2.1. Ox-tallow homogeneous triacylglycerols

The extensive fragmentation study of ox tallow TAGs was investigated to elucidate the TAG structures. When performing the IRMPD fragmentation of the homogeneous TAG tristearin (SSS) at m/z 897.8466 (Δm = 0.33 ppm, Fig. 5), only the ion issued from the loss of the free fatty acid RCH_2CO_2H from the parent ion $[M + Li]^+$ giving the ions $[M + Li\text{-}RCH_2CO_2H]^+$ at m/z 613.5750 (Δm = 0.32) is observed. The identity of the fatty acid substituents in TAG species can also be deduced by monitoring the $[RCH_2CO_2H + Li]^+$ fragment ions at m/z 291.2875 (Δm = 0.12 ppm) in the low mass range of the MS/MS spectrum.

3.2.2. Ox-tallow heterogeneous triacylglycerols

TAGs containing two different fatty acid substituents present a slightly more complicated MS/MS spectrum. Each acylating fatty acid moiety generates three groups of ions (i) the first group is represented by $[M + Li\text{-}R_nCH_2CO_2H]^+$ ions and results from the loss of one fatty acid group; (ii) the second group traduces the successive loss of two carboxylic acid moieties, and (iii) the last group reflects the nature of each fatty acid moiety as $[RCH_2CO_2H + Li]^+$ ion is represented (see supplementary data). Focusing on the main TAG referred to ECN 50 (see Fig. 4(A)), i.e., the monounsaturated TAGs 50:1 (named 1,2-dipalmitoyl-3-oleoylglycerol, noted PPO) and its regioisomer (named 1,3-dipalmitoyl-2-oleoylglycerol, noted POP), it can be pointed out that the fragmentation spectrum (Fig. 6(A)) presents a molecular lithiated ion at m/z 839.6738 (Δm = 0.47 ppm) giving peaks at m/z 583.5276 (Δm = −0.35 ppm) and at m/z 557.5119 (Δm = −0.49 ppm) by loss of free palmitic or oleic acid respectively (Fig. 6(B)). The former ion $[M + Li\text{-}C_{15}H_{31}CO_2H]^+$ at m/z 583.5276 can lose an α,β-unsaturated oleic or palmitic acid moiety, respectively giving the ion $[M + Li\text{-}C_{15}H_{31}CO_2H\text{–}C_{15}H_{29}CH{=}CH\text{–}CO_2H]^+$ at m/z 303.2877 (Δm = 0.41 ppm), and the ion $[M + Li\text{-}C_{15}H_{31}CO_2H\text{–}C_{13}H_{27}CH{=}CH\text{–}CO_2H]^+$ at m/z 329.3030 (Δm = 0.05 ppm) (Fig. 6(C)). Both palmitic and oleic substituent's are also directly identified as lithiated ion $[RCH_2CO_2H + Li]^+$ at m/z 263.2562 (Δm = −0.08 ppm) and 289.2719 (Δm = 0.07 ppm), respectively. The ions detected at m/z 261.2405 (Δm = −0.37 ppm) and 319.2824 (Δm = −0.04 ppm) are respectively attributed to the ions $[M + Li\text{-}R_3CH_2CO_2H\text{-}R_1CH_2COO\text{–}CH_2\text{–}CH{=}CH_2]^+$ and $[M + Li\text{-}R_{2/1}CH_2CO_2H\text{-}R_{1/2}CH{=}C{=}O]^+$ for the triacylglycerol PPO. The ion at m/z 345.2982 (Δm = 0.31 ppm) corresponds to $[M + Li\text{-}R_2CH_2CO_2H\text{-}R_3CH{=}C{=}O]^+$ and $[M + Li\text{-}R_3CH_2CO_2H\text{-}R_1CH{=}C{=}O]^+$ (Fig. 6(C)). The ion $[M + Li\text{-}R_3CH_2CO_2H\text{-}R_1CH_2COO\text{–}CH_2\text{–}CH{=}CH_2]^+$ reveals that lithiated TAGs can lose their two outer fatty acid substituent's (sn-1 and sn-3). This pathway is minor comparing to the fragmentation involving an outer substituent and its adjacent sn-2 moiety.

A similar analysis can be applied to the isobar TAGs 52:1 at m/z 867.7052 (Δm = −0.34 ppm) from ox-tallow that contains three different fatty acid substituents. The main fragment ions at m/z 583.5274 (Δm = −0.70 ppm), 585.5440 (Δm = −0.85 ppm)

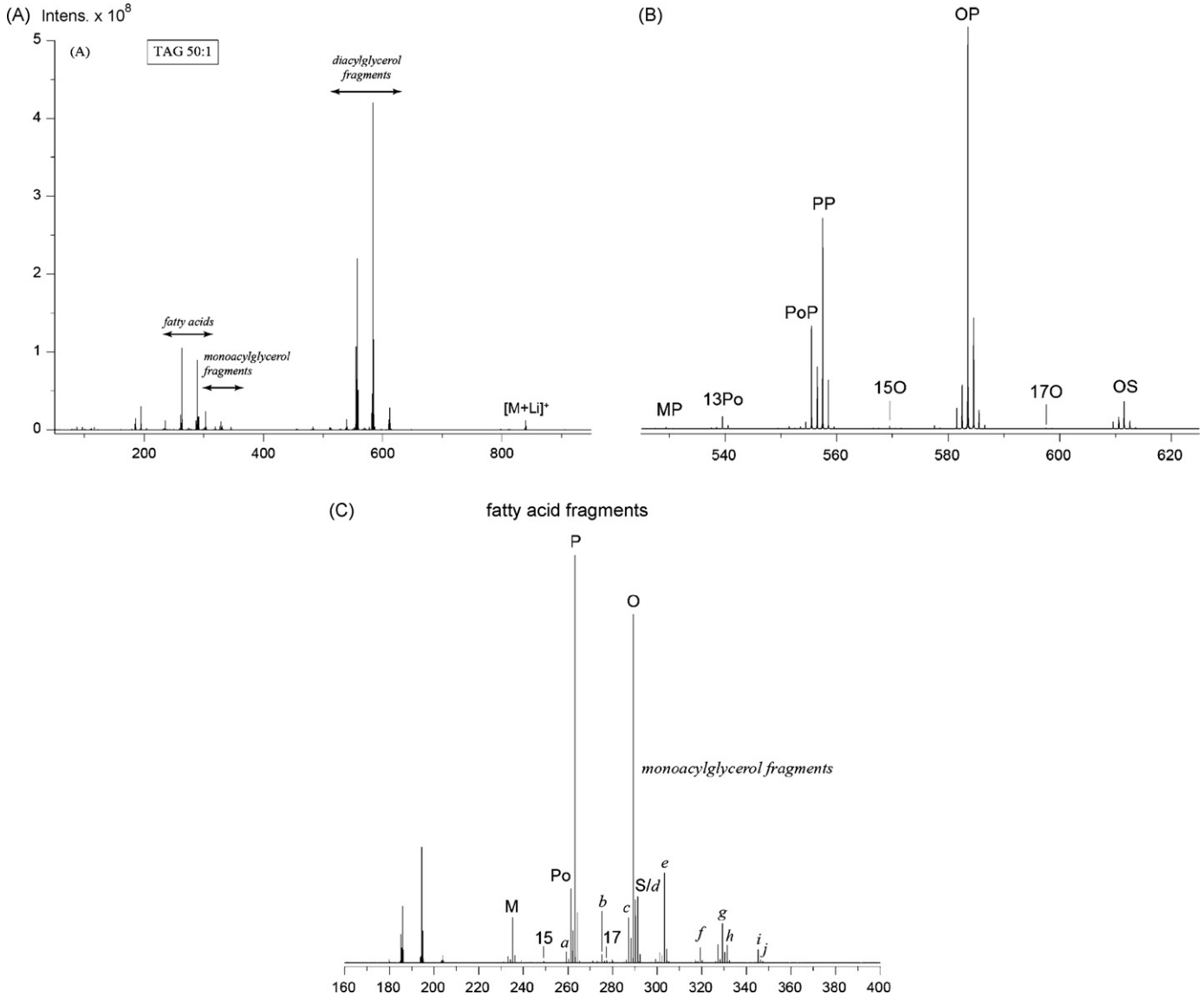

Fig. 6. (A) IRMPD MS/MS profiles of the ion $[M+Li]^+$ at m/z 839.6738 from ox tallow TAGs extract corresponding mainly to PPO and POP TAGs (50:1), (B) zoom on the diacylglycerol fragments, (C) zoom on the low molecular weight mass range.
The abbreviation details are specified in Table 2. The fragment ions written in italics refer to the successive loss of two fatty acids. The ions noted *e* and *f*, generated by the loss of neutral oleic acid and palmitic acid in ketene form, reflect the presence of the two regioisomers OPP and POP. The ion noted a, formed by the loss of neutral palmitic acid and oleate allyl ester, affords to distinguish the regioisomer OPP. The ions noted *b* and *d* are common to the three isomers MOS, MSO and OSM; the ions noted *h* and *j* are specific to the isomer MOS.

and 611.5582 ($\Delta m = -1.47$ ppm) (Fig. 7), correspond to $[M+Li\text{-}RCH_2CO_2H]^+$ (with RCH_2CO_2H representing P, O or S), and are common to both triacylglycerols PSO and POS. Additionally, palmitic, stearic and oleic substituent's are also identified as lithiated ion $[RCH_2CO_2H+Li]^+$ at m/z 263.2562, 291.2875 and 289.2719 respectively ($\Delta m = 0.08/0.01/0.07$ ppm). The presence of the ions at m/z 329.3033 ($\Delta m = 0.25$ ppm) and 345.2982 ($\Delta m = 0.42$ ppm) reveals the presence of the isomer PSO (Fig. 7 and supplementary data). The first one is formed either by the loss of a neutral palmitic acid $C_{15}H_{31}CO_2H$ thus an α,β-unsaturated stearic acid $C_{15}H_{31}–CH{=}CH_2–CO_2H$, or by the loss of a neutral stearic acid $C_{17}H_{35}CO_2H$ followed by α,β-unsaturated palmitic acid $C_{13}H_{27}–CH=CH_2–CO_2H$; the latter at m/z 345.2982 is generated by the successive loss of a stearic acid and palmitic in its ketene form $C_{14}H_{29}–CH{=}C{=}O$. In opposition, the corresponding ions at m/z 331.3193 ($\Delta m = 1.25$ ppm) and 347.3144 ($\Delta m = 1.72$ ppm), generated by the three same fragmentation ways from the regioisomer POS, are minor or absent, concluding that the main regioisomer is PSO, although POS is presence as traces.

Globally, the main TAG markers identified in ox tallow and their fragmentations (see supplementary data) constitutes our database for archaeological MS and MS/MS spectra interpretations providing specific information on the species analyzed.

3.3. Application of lipidomics to archaeological lamps

The nine sherds of lamps studied were chosen among the material excavated from 1991 to 2006. As any ceramics presented visible organic deposit on its inner side, the only chemical information could be obtained from the organic matter trapped and present as an impregnation of the porous clay matrix of the ceramic.

In a first step, the total lipid extracts of the nine sherds were analyzed by HRGC-EIMS in order to verify the presence of preserved organic matter, and to identify low- and medium-molecular weighted compounds (data not shown). Six samples presenting a

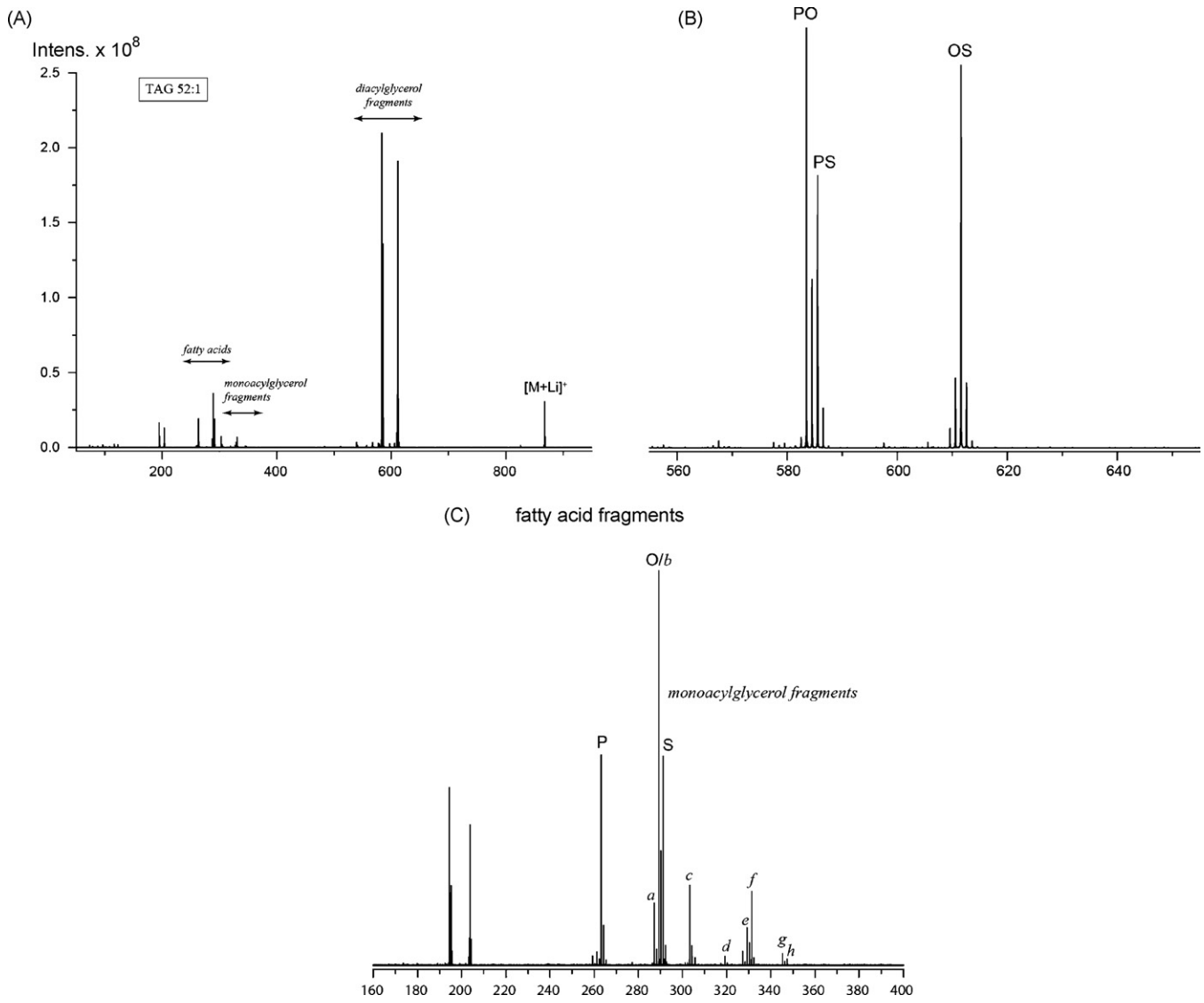

Fig. 7. (A) IRMPD MS/MS profiles of the ion $[M+Li]^+$ at m/z 867.7052 from ox tallow TAGs extract corresponding to PSO and POS TAGs (52:1), (B) zoom on the diacylglycerol fragments, (C) zoom on the low molecular weight mass range. The ions noted *c* and *d* are generated by the loss of oleic acid and α,β-unsaturated stearic acid, or of stearic acid and α,β-unsaturated oleic acid. The ions *b* and *e* are specific to PSO. The ions *a* and *f* reveal the presence of the isomer POS.

high concentration in free fatty acids, in mono- or diacylglycerols, and/or in sterols were selected. Their lipidic extracts were purified on SPE procedure on diol-cartridge in order to separate and concentrate the native triacylglycerols. The purified TAG fractions were analyzed according to the same conditions than those used for modern fats. Fig. 8 shows the MS profile of the native TAGs from the lamp X4. The other six profiles observed were very similar and reveals the same markers. The profile is characterized by a large distribution of TAGs corresponding to triacylglycerols with ECN from 46 to 57. Considering the organic material trace content and the advanced degradation state of this sample, very good signal to noise ratio of the MS spectrum can be observed. Globally, the higher peak intensities are even-C-numbered TAGs, from TAG 46:0 to TAG 56:0 with the TAG 52:0 as main marker. Among these even-C-numbered TAGs, odd-C-numbered TAGs are detected from TAG 47:0 to TAG 57:0. If the environmental conditions have guaranteed the preservation of some native TAGs against hydrolytic degradation, the spectrum reveals a strong dominance of saturated TAGs, a weak proportion of monounsaturated TAGs, e.g., TAG 50:1, 52:1 or 54:1 and the global disappearing of polyunsaturated TAGs. These saturated TAGs were already highlighted in organic residues stuck preserved on the inner surface of the canopic jar D with the monogram of Ramses II [36] and in a ceramic potsherd from Sagalassos [5]. In fact, these profiles characterized by high proportion of saturated TAGs can be explained with the high sensitivity of unsaturated fatty acids to oxidation processes, especially in the presence of oxidoreductive catalyst such transition metal ions commonly present in the clay [10,37]. Consequently, these compounds are more polar and are easily lixiviated by running water. These results, directly transposable to fatty acid substituents in TAGs, can explain the modification of the initial pattern and the preferential loss of polyunsaturated TAGs in the oxidative context of Olbia.

The chemical structure of the main markers is investigated using IRMPD. For example, the Fig. 9 presents the MS/MS spectrum of the lithiated adduct $[M+Li]^+$ at m/z 869.7208 ($\Delta m = -0.34$ ppm). The ion at 613.5741 ($\Delta m = -0.11$ ppm) results from the neutral palmitic acid loss. The ions at m/z 303.2870 ($\Delta m = -1.64$ ppm) and at m/z 331.3193 ($\Delta m = 1.51$ ppm) were obtained by octadec-2-enoic acid or hexadec-2-enoic acid loss respectively. The precursor ion loses also a stearic acid giving the ion at m/z 585.5439 ($\Delta m = 0.85$ ppm); this last ion losing the neutral fragment $C_{13}H_{27}CH{=}CH_2{-}CO_2H$ to form the ion at m/z 303.2870 identifying the TAGs SSP and SPS.

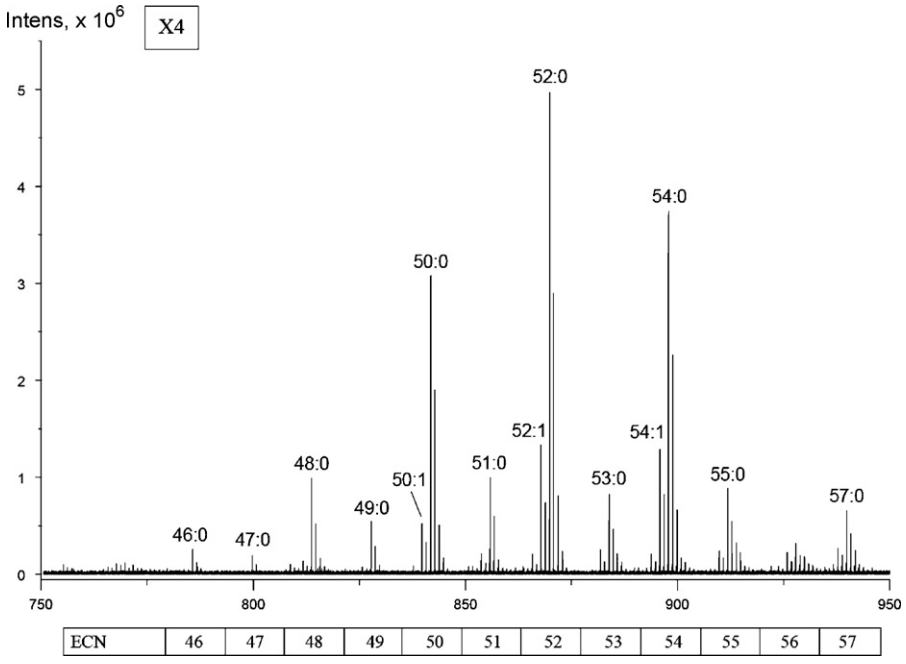

Fig. 8. MS profiles of the TAG fractions from the Olbia lamp X4.

Globally, the mass profiles of the archaeological extracts show an alternation between major series of even carbon-numbered TAGs, and minor series of odd carbon numbered TAGs. The MS/MS profiles of odd TAGs reveal the presence of odd-numbered fatty acids moieties for the minor compounds, e.g., pentadecanoic or heptadecanoic acid moieties, characteristic of the rumen bacteria [31]. The comparison of MS and MS/MS profiles of reference fats extracted from the adipose tissues shows that only bovine or ovine species present such odd carbon-numbered series, e.g., TAGs containing one odd carbon-numbered fatty acid moiety. The identification of odd carbon-numbered series in the archaeological extracts allows concluding to the presence of bovine or ovine fats in the Olbia lamps showing that the population preferred elaborating fuel from local bovine or ovine species than to import olive oil from the South provinces.

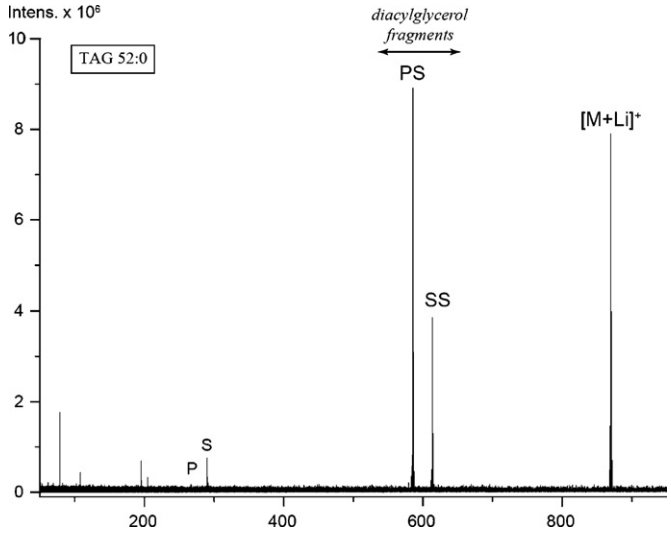

Fig. 9. IRMPD MS/MS profiles of the ion $[M+Li]^+$ at m/z 869.7208 from the Olbia lamp X4 TAGs extract corresponding to SSP and SPS TAGs (52:0).

4. Conclusion

Although gas chromatographic analysis, using flame ionization detection or coupled with mass spectrometry, is the most common analytical tool for the study of organic archaeological remains preserved in ceramics, the use of MS and MS/MS-based technique with a nanoelectrospray source has significant potential for extending our knowledge about the structure of the soluble high-molecular-weighted constituents. The implemented cationization of the lipidic extract by lithium ion induces a powerful enhancement of the sensitivity and selectivity of the analysis, inducing the possibility to implement the method to precious trace archaeological samples. The IRMPD spectra of the lithiated TAGs reveal fragmentation reactions including loss of free neutral fatty acid and loss of fatty acid as α,β-unsaturated moieties. The access to the native structure brings more valuable information allowing distinction between oils, fats and dairy products from different origins (plants, mammals, etc.). Using adapted sample preparation conditions to trace samples in advanced degradation state, including lipidic extraction with dichloromethane/methanol mixture and additional ultrasonication treatment, purification using diol cartridge and nanoESI analysis protocols well-adapted, the present analysis succeeds identifying the nature of fats used as fuel used in Olbia lamps. From an historical point of view, these results provide interesting new data, completing the hypothesis formulated by archaeologists about the use of local fatty materials.

Acknowledgment

This work was funded by the Agence Nationale de la Recherche ANR-08-JCJC-0082-01. The Proteomics core facility and the FT-ICR mass spectrometer used in this study were funded by the European Community (FEDER), the Région Nord-Pas de Calais (France), the Génopole of Lille, the CNRS, and the Université des Sciences et Technologies de Lille.

Appendix A. Supplementary data

Supplementary data associated with this article can be found, in the online version, at doi:10.1016/j.ijms.2009.03.003.

References

[1] R. Garcia Gimenez, R. Vigil de la Villa, M.D. Petit Dominguez, M.I. Rucandio, Talanta 68 (2006) 1236–1246.
[2] S. Passi, M.C. Rothschild-Boros, P. Fasella, M. Nazzaro-Porro, D. Whitehouse, J. Lipid Res. 22 (1981) 778–784.
[3] M.P. Colombini, G. Giachi, F. Modugno, E. Ribechini, Microchem. J. 79 (2005) 83–90.
[4] M.S. Copley, H.A. Bland, P. Rose, M. Horton, R.P. Evershed, Analyst 130 (2005) 860–871.
[5] K. Kimpe, P.A. Jacobs, M. Waelkens, J. Chromatogr. A 937 (2001) 87–95.
[6] N. Garnier, C. Tokarski, C. Rolando. In: Salles, J.-F. (Ed.), Lampes antiques du Bilad esh-Sham, de l'Âge du Bronze à la période de transition byzantine-ommeyyade, IFPO Amman, Amman, Petra 2008.
[7] N. Garnier, C. Cren-Olivé, C. Rolando, M. Regert, Anal. Chem. 74 (2002) 4868–4877.
[8] M.P. Colombini, F. Modugno, E. Ribechini, J. Mass Spectrom. 40 (2005) 890–898.
[9] H.-D. Belitz, W. Grosch, P. Schieberle, Food Chemistry, Springer-Verlag, Berlin, 2004.
[10] M. Stratakis, M. Orfanopoulos, Tetrahedron 56 (2000) 1595–1615.
[11] A. Staby, J. Mollerup, Fluid Phase Equilib. 91 (1993) 349–386.
[12] P. Sandra, A. Medvedovici, Y. Zhao, F. David, J. Chromatogr. A 974 (2002) 231–241.
[13] V. Ruiz-Gutierrez, L.J.R. Barron, J. Chromatogr. B 671 (1995) 133–168.
[14] T. Kusaka, S. Ishihara, M. Sakaida, A. Mifune, Y. Nakano, K. Tsuda, M. Ikeda, H. Nakano, J. Chromatogr. A 730 (1996) 1–7.
[15] H.R. Mottram, S.E. Woodbury, R.P. Evershed, Rapid Commun. Mass Spectrom. 11 (1997) 1240–1252.
[16] W.C. Byrdwell, W.E. Neff, Rapid Commun. Mass Spectrom. 16 (2002) 300–319.
[17] A. Jakab, I. Jablonkai, E. Forgács, Rapid Commun. Mass Spectrom. 17 (2003) 2295–2302.
[18] L. Mondello, P.Q. Tranchida, V. Stanek, P. Jandera, G. Dugo, P. Dugo, J. Chromatogr. A 1086 (2005) 91–98.
[19] M. Holcapek, M. Lísa, P. Jandera, N. Kabátová, J. Sep. Sci. 28 (2005) 1315–1333.
[20] P. Dugo, T. Kumm, M. Lo Presti, B. Chiofalo, E. Salimei, A. Fazio, A. Cotroneo, L. Mondello, J. Sep. Sci. 28 (2005) 1023–1030.
[21] P. Dugo, T. Kumm, M.L. Crupi, A. Cotroneo, L. Mondello, J. Chromatogr. A 1112 (2006) 269–275.
[22] S.-S. Cai, L.C. Short, J.A. Syage, M. Potvin, J.M. Curtis, J. Chromatogr. A 1173 (2007) 88–97.
[23] S.-S. Cai, J.A. Syage, J. Chromatogr. A 1110 (2006) 15–26.
[24] S.-S. Cai, J.A. Syage, Anal. Chem. 78 (2006) 1191–1199.
[25] K. Kimpe, P.A. Jacobs, M. Waelkens, J. Chromatogr. A 968 (2002) 151–160.
[26] N. Garnier. In: Michel Bonifay, J.-C. T. (Ed.), LRCW2. Late Roman Coarse Wares, Cooking Wares and Amphorae in the Mediterranean: Archaeology and Archaeometry, Archaeopress, British Archaeological Reports, MMSH, 2007, pp. 39–58.
[27] S. Mirabaud, C. Rolando, M. Regert, Anal. Chem. 79 (2007) 6182–6192.
[28] J.K.S. Møller, R.R. Catharino, M.N. Eberlin, Food Chem. 100 (2007) 1283–1288.
[29] F.-F. Hsu, J. Turk, J. Am. Soc. Mass Spectrom. 10 (1999) 587–599.
[30] J. Folch, M. Lees, G.H.S. Stanley, J. Biol. Chem. 226 (1957) 497–509.
[31] M.C. Perez-Camino, W. Moreda, A. Cert, J. Chromatogr. A 721 (1996) 305–314.
[32] N. Garnier, Analyse structurale de matériaux organiques conservés dans des céramiques antiques. Apports de la chromatographie et de la spectrométrie de masse. Université Pierre et Marie Curie (Paris VI), Paris, 2003.
[33] W. Zhigang, R.P. Rodgers, A.G. Marshall, J. Agric. Food Chem. 52 (2004) 5322–5328.
[34] O.F. Van den Brink, J.J. Boon, P.B. O'Connor, M.C. Duursma, R.M.A. Heeren, J. Mass Spectrom. 36 (2001) 479–492.
[35] B. Vlaeminck, V. Fievez, A.R.J. Cabrita, A.J.M. Fonseca, R.J. Dewhurst, Anim. Feed Sci. Technol. 131 (2006) 389–417.
[36] A. Charrié-Duhaut, J. Connan, N. Rouquette, P. Adam, C. Barbotin, M.F. de Rozieres, A. Tchapla, P. Albrecht, J. Archaeol. Sci. 34 (2007) 957–967.
[37] A.W. Girotti, J. Photochem. Photobiol. B: Biol. 63 (2001) 103–113.